Comparison of Theory and Experiment for Propfan Inlets

Victor Lyman* and John P. Hancock†
Lockheed-Georgia Company, Marietta, Georgia

Studies have indicated that the use of propfans can result in fuel savings of 20–25% relative to turbofans. Therefore, a program was initiated to perform wind-tunnel tests on a series of inlet models for advanced tractor, turboprop installations. Single-scoop, twin-scoop, and annular inlets were tested to obtain inlet pressure recovery and distortion, external cowl surface pressures, external cowl forebody drag, and propeller blade stress data. An analysis was undertaken for each of the propfan inlet configurations tested using Lockheed's QUADPAN panel program. Calculated nacelle surface pressures correlate well with experiment, except where Mach number is high or viscous effects predominate. The effect of the inlet interference flowfield on the propeller was calculated using Lockheed's PROPVRTX propeller analysis program. The results showed that displacing the inlet in the aft direction reduced the adverse effects on the propeller cyclic stresses. Measured propeller stress data support these results. It is concluded that inlet/cowl designs can be assessed by computational methods.

Introduction

STUDIES have indicated that the use of propfans can result in fuel savings of 20–25% relative to turbofans. Therefore, a program was initiated to perform wind-tunnel tests on a series of inlet models for advanced tractor, turboprop installations. This effort was a joint program involving Lockheed-Georgia Company, United Technologies (Pratt & Whitney Aircraft and Hamilton Standard), and NASA Lewis, which became known as the GUN program. Single-scoop and twin-scoop inlets, with and without a boundary-layer diverter, and an annular inlet were tested to obtain inlet pressure recovery and distortion, external cowl surface pressures, external cowl forebody drag, and propeller stress data. The single-scoop inlet with a boundary-layer diverter was also tested at two axial positions relative to the propfan. All the inlets were tested over a range of Mach numbers from 0.2 to 0.8 and a range of mass flow ratios. The results of these tests have been reported in detail,[1] as have the design methodology and previous theoretical analysis of the inlets.[2,3]

Since wind-tunnel testing is very expensive, there is a need to make use of validated computational methods to predict flowfields and surface pressures for propfan inlets, especially in optimizing their design. Since testing in the GUN program provides an excellent data base with which to correlate computational methods, an analysis was undertaken for four of the tested propfan nacelle-inlet configurations. The configurations were modeled using Lockheed's QUADPAN panel program,[4] and external cowl surface pressures were calculated. This paper presents the results of the analyses and their correlations with experimental data. The application of computational methods as a design tool is demonstrated.

Presented as Paper 86-1628 at the AIAA/ASME/SAE/ASEE 22nd Joint Propulsion Conference, Huntsville, AL, June 16–18, 1986; received Sept. 9, 1986; revision received March 6, 1987.

*Specialist Engineer, Propulsion, Flight Sciences Division. Associate Fellow AIAA.

†Staff Engineer, Flight Sciences Division.

Theoretical Analysis

Theoretical analysis of the propfan inlets was conducted using Lockheed's advanced low-order three-dimensional panel method—QUADPAN. The unique features of QUADPAN allow adequate representation of the complex inlet geometries and the ability to concentrate panels in areas with rapidly changing geometric curvature and consequent high-pressure gradients. They also facilitate working with nacelle-inlet geometries that are defined on the CADAM system. For the propfan inlet models, the geometric data were supplied through the CADAM system from loft data used to generate the original wind-tunnel models. This assured accurate modeling of the geometry with sufficient paneling to give detailed surface pressures.

QUADPAN solves the Prandtl-Glauert equation for inviscid, linearized compressible flow. Therefore, it is applicable for subsonic Mach numbers and will provide good correlation with experimental data as long as shocks are not present and viscous effects are not dominant. It is also applicable to inlet duct flows. Although internal inlet performance is not analyzed in this paper, the ability to model the inlet duct is essential in order to set the inlet mass flow and properly model spillage over the cowl external surface.

One of the advantages of the QUADPAN code, particularly in handling inlet duct flows, is its formulation of the boundary conditions. QUADPAN uses an internal potential boundary condition; i.e., the perturbation potential inside the body surface is set to zero. This makes the solution less sensitive to paneling variation and reduces panel leakage for internal flows. In addition, with the use of permeable panels, it is possible to specify the first-order mass flux for the inlet internal flow plane, which corresponds to the engine compressor face. For incompressible flow, or even low Mach number flows, one can specify the mass flow under this condition simply by specifying the velocity. At higher Mach numbers, however, this causes errors because of the linearization assumptions in the boundary conditions. Typically, mass flow ratios higher than desired must be specified in order to solve for desired velocities across the permeable panel.

The version of the QUADPAN program used in this study includes a rigid propeller slipstream model, which uses Goldstein's classical vortex theory to predict the propeller-induced axial and tangential velocities anywhere in the pro-

peller slipstream. This is accomplished through input of experimentally determined distributions of axial and tangential velocities just aft of the propeller plane. By modeling the slipstream with a semi-infinite, helical vortex system and applying the continuity principle, the theory calculates the slipstream contraction, local radius, and axial velocity for a point on the nacelle surface and applies axial and tangential velocity as a boundary condition. Tangential velocity is assumed to have the same profile downstream as it does at the propeller. As there is a pressure rise through the propeller disk that comes from the addition of energy by the propeller, it is necessary to include this explicitly in the calculation. The pressure rise can be expressed in terms of the velocity of the fully contracted slipstream.

Lockheed's PROPVRTX program,[5] a propeller analysis program based on classical vortex theory, is used in the study of propeller/nacelle interactions. Corrections for finite blade width, thickness, and compressibility are included. PROPVRTX predicts the slipstream properties produced by a propeller of given geometry and advance ratio. The undisturbed slipstream is defined by its boundary shape and the radial distribution of the local vorticity, induced velocity, and swirl angle. The code can also analyze propellers in a spatially nonuniform flowfield and provide the change in propeller performance as influenced by the inlet interference flowfield.

Experimental Setup

Propfan

The inlets were tested with a 24.5-in.-diam variable-pitch model of the eight-bladed SR-3 propfan, which was designed by Hamilton Standard.[6] Figure 1 shows the propeller with the nacelle and single-scoop inlet with boundary-layer diverter mounted on the propeller test rig (PTR) in the United Technologies Research Center (UTRC) wind tunnel. The direction of rotation of the propeller is counterclockwise, looking forward.

For blade stress tests, a slip-ring assembly was installed on the nose of the spinner to transfer the strain-gage signals from rotating to stationary hardware. A sting on the axis of rotation carried the wiring upstream to a low-velocity section for exit from the tunnel.

Nacelle and Inlets

Three basic types of propfan inlets were tested under the GUN program: an axisymmetric annular inlet, a single-scoop inlet with and without boundary-layer diverter, and a twin-scoop inlet with and without boundary-layer diverter. Panel models of five inlets that will be considered in the following analyses are shown in Fig. 2. The single-scoop inlet with the boundary-layer diverter is shown in two versions, with the inlet located in a forward position and in an aft position (respectively, 11 and 20% in terms of propeller diameters aft of the propeller axis).

The test was conducted in three phases, with pressure measurements on the single-scoop inlets in GUN-I, thrust-minus-drag and cowl drag measurements in GUN-II, and pressure and drag measurements on the remaining inlets in GUN-III. The inlet airflow was aspirated through a faired duct to the flow control measurement section and exhaust system under the floor. After GUN-I, these inlets were rebuilt with an internal balance that measured the axial aerodynamic force on the inlet forebody. For this setup, a flow-through arrangement, with variable exit nozzle areas, replaced the ducted exhaust. A similar cowl drag balance arrangement was fabricated for the twin-scoop and annular inlets.

Instrumentation

The models incorporated extensive, steady-state, static, and total pressure instrumentation. These are identified in Fig. 3 for the single-scoop inlet with boundary-layer diverter. The propeller drive motors, their associated drive train, and the entire nacelle front end are metric. In addition, the cowling, which consists of the forward nacelle aft of the spinner, and inlet fairing, is metric on a special cowl drag balance. Internal cavity pressure is measured to supply the required tare correction. Use of the cowl drag balance provided the means whereby cowl drag and, eventually, spinner drag could be separated out from total front-end thrust minus drag.

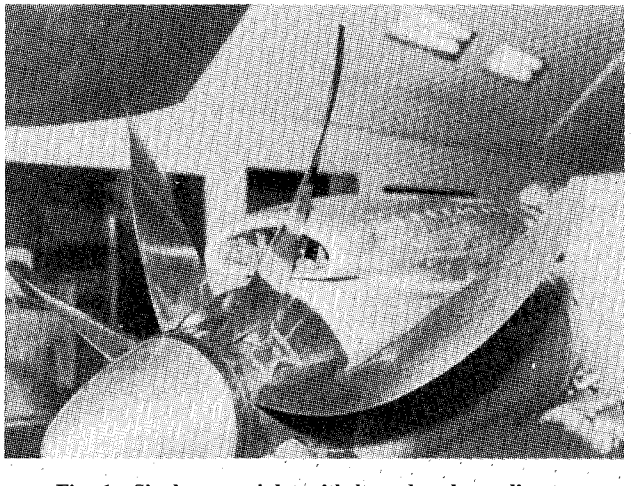

Fig. 1 Single-scoop inlet with boundary-layer diverter.

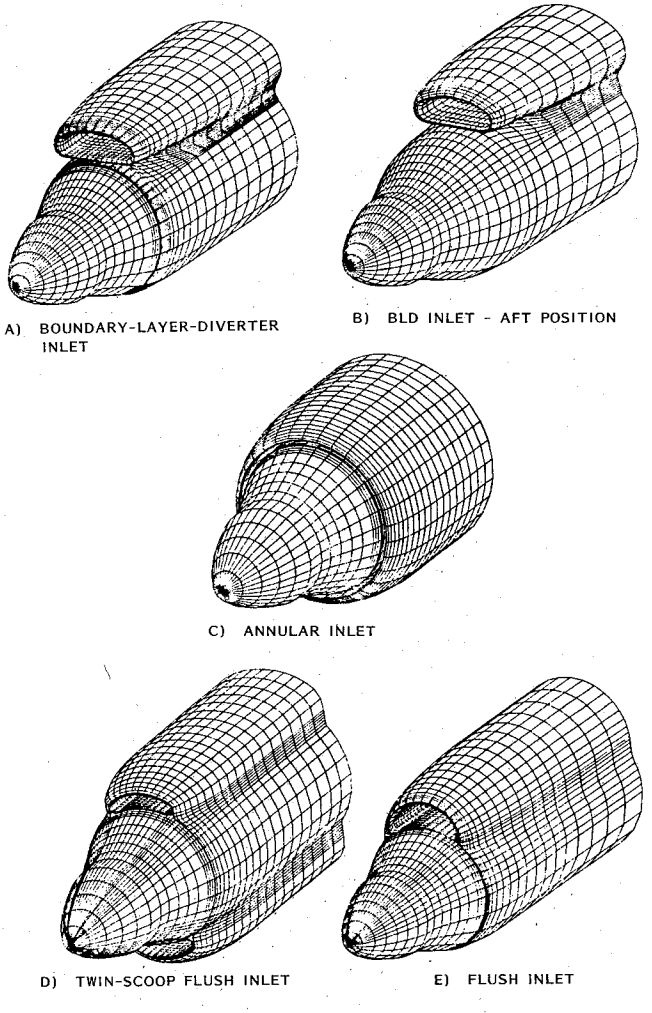

Fig. 2 Propfan-nacelle configuration panel models.

Wind Tunnel

The test program was conducted in the UTRC large subsonic wind tunnel. The tunnel is a single-return, closed-throat facility with interchangeable 8- and 18-ft octagonal test sections. The main drive system is a 9000-hp synchronous motor with a variable-speed coupling driving a 26-ft-diam, 20-blade fan. The 8-ft test section used in the GUN tests is inserted in the 18-ft section and provides speeds up to Mach 0.90. The tunnel operates with atmospheric stagnation pressure and closely controlled stagnation temperature.

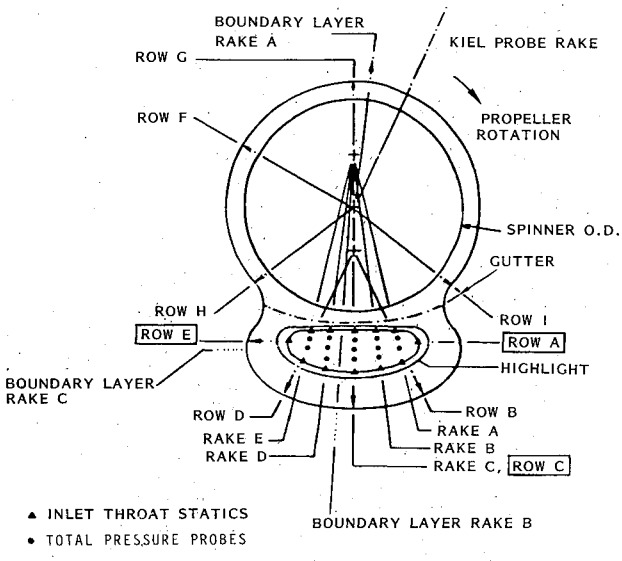

Fig. 3 Static pressure orifice locations.

Propeller Test Rig

The propeller test rig consists of two variable-speed motors in tandem in a streamlined pod and pylon. Each motor is rated at 375 hp at 12,000 rpm. Together they provide a maximum torque of 330 ft-lb over the entire speed range. The stators for the motors are supported on hydrostatic bearings that allow free axial and rotational movement. Pressures in the pod and on its external surfaces are measured and used to correct the axial thrust reading for unbalanced pressures on test-rig components.

Correlation of Surface Pressures

The three basic types of propfan inlets mentioned previously were modeled with the QUADPAN program, and theoretical predictions were made to assess the propeller-induced effects, mass flow ratio effects, and Mach number effects. Correlation of external surface pressures is presented for the axisymmetric inlet in Fig. 4 with and without the propeller for mass flow ratios of 0.60 and 0.85. These are based on inlet throat area. The effect of increasing mass flow ratio, which reduces spillage and velocities over the inlet, is properly predicted by the theory. No effect of adding the propeller can be discerned from the theoretical prediction, as the height of the inlet is so small that it ingests only the flow induced by the root sections of the propeller. As the experimental results show, velocities over the inlet are actually reduced because of the thick propeller-hub boundary layer produced by strong hub/blade interactions. Also, for this reason, correlation farther back on the external cowl surface is not as good as that observed for the other inlets.

Correlations are presented in Fig. 5 for the flush single-scoop inlet. These show external cowl surface pressures on the top and sides of the scoop, with and without the propeller. The propeller-off data show excellent correlation with experiment. Good correlation has also been obtained for the propeller-on case, although pressure coefficients are somewhat overpredicted on the windward side, possibly due to a localized unsteady propeller/inlet interaction effect. The

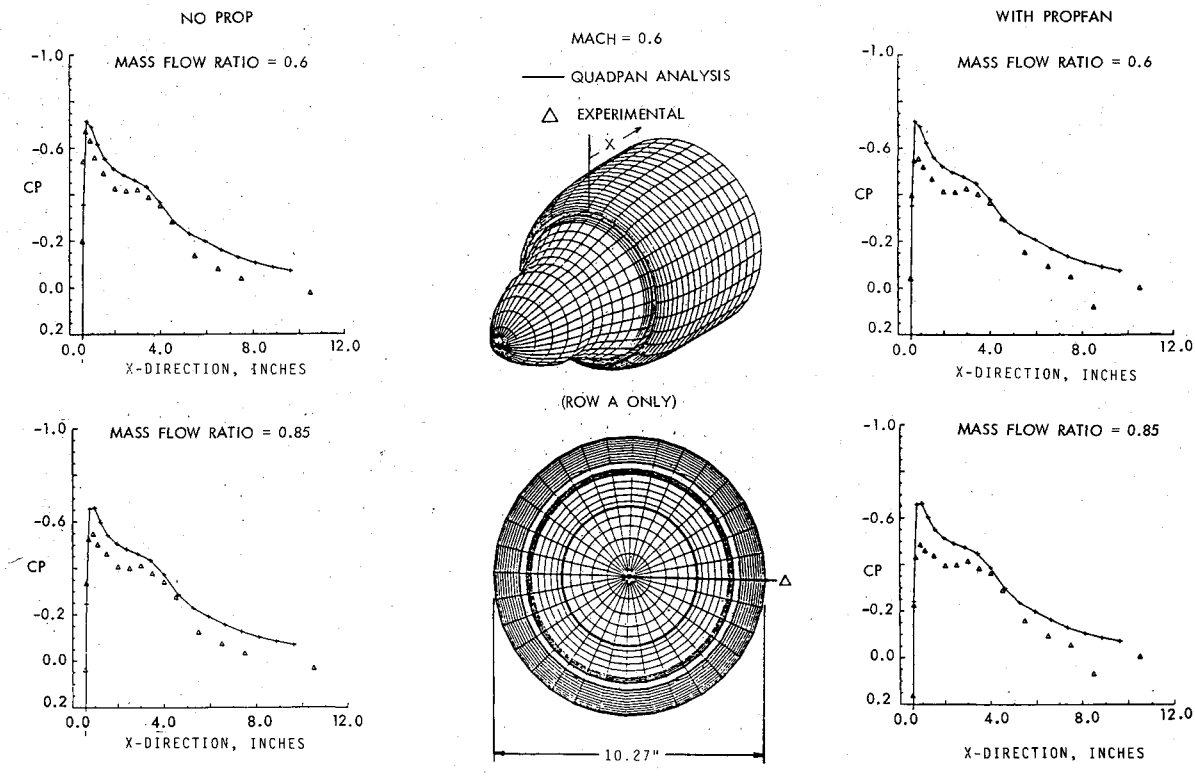

Fig. 4 Pressure distributions for axisymmetric inlet.

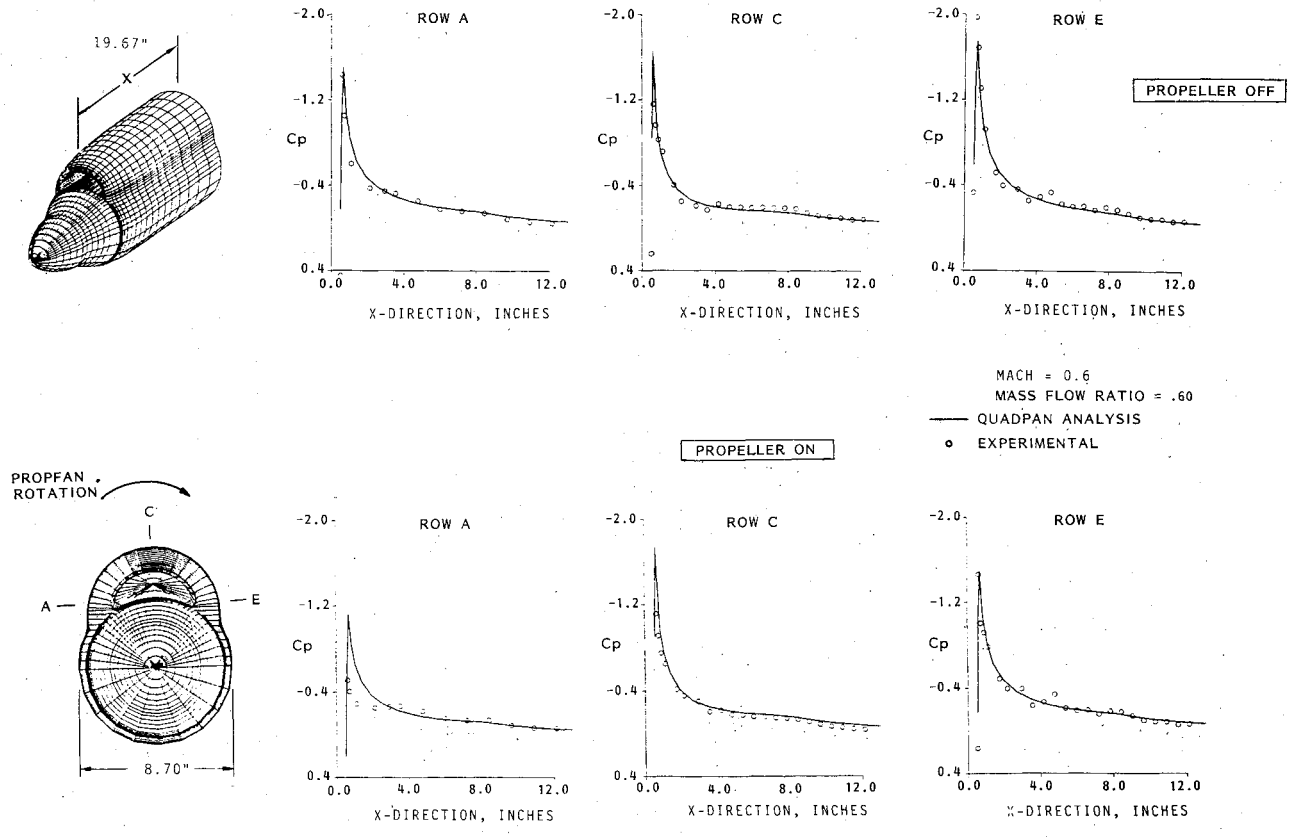

Fig. 5 Pressure distributions for flush single-scoop inlet.

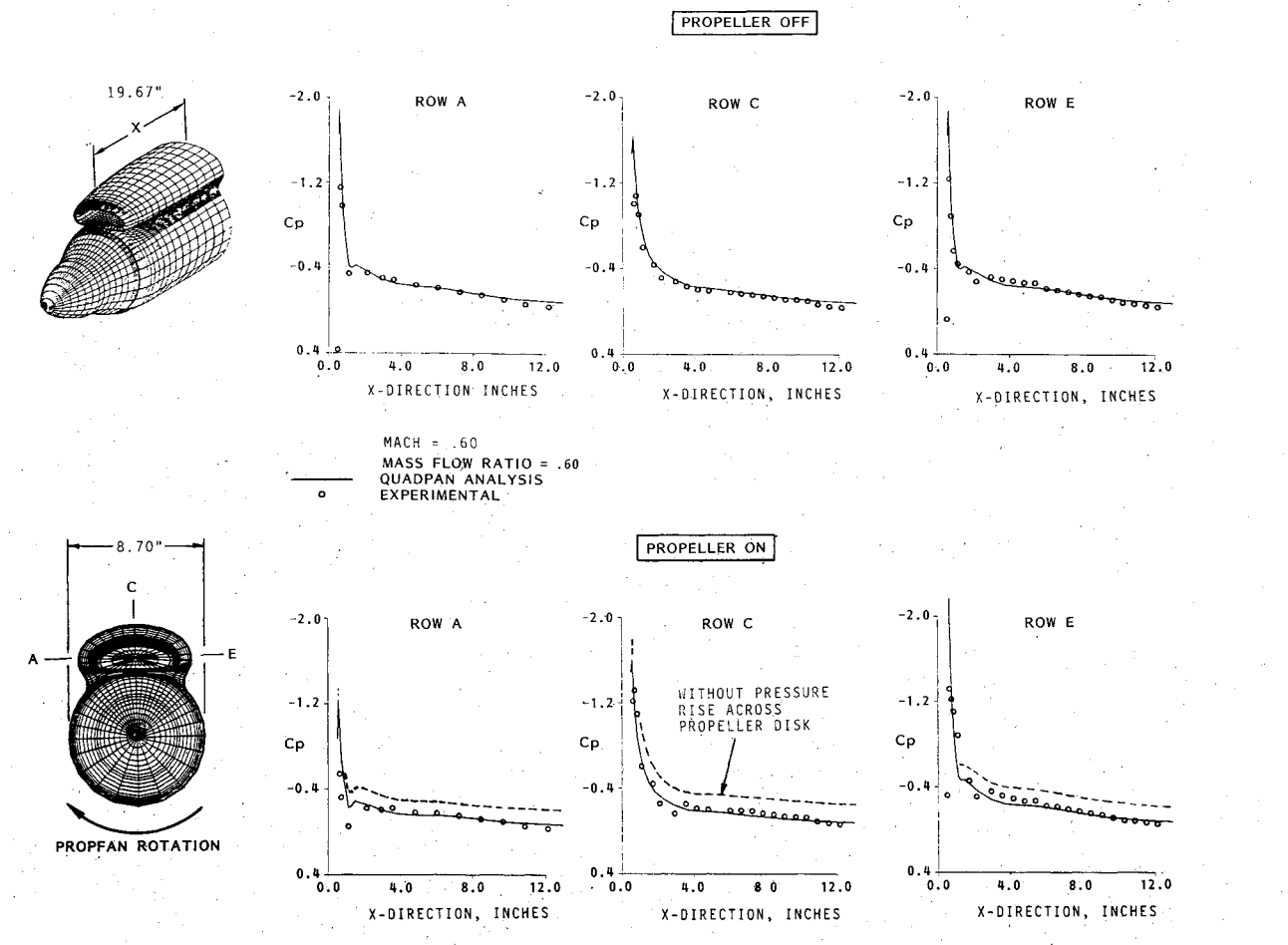

Fig. 6 Pressure distributions for single-scoop inlet with boundary-layer diverter.

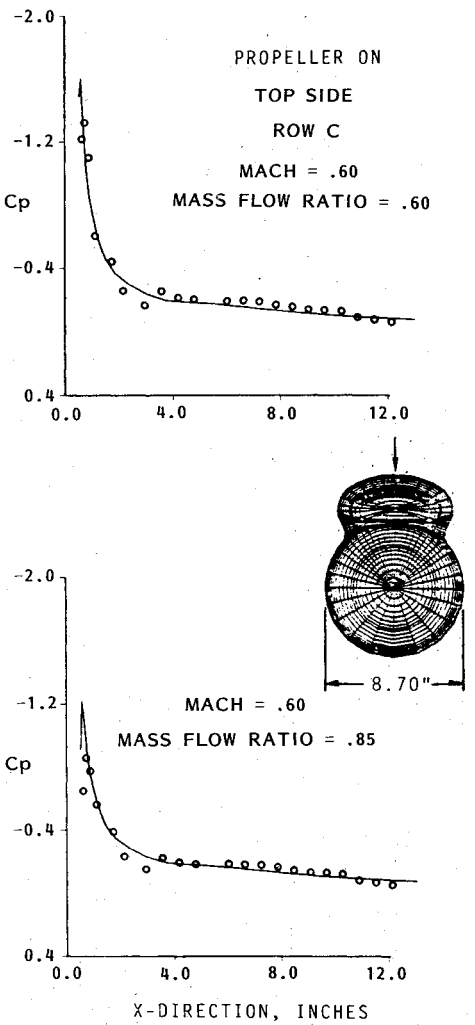

Fig. 7 Pressure distributions for single-scoop inlet with boundary-layer diverter, effect of mass flow ratio.

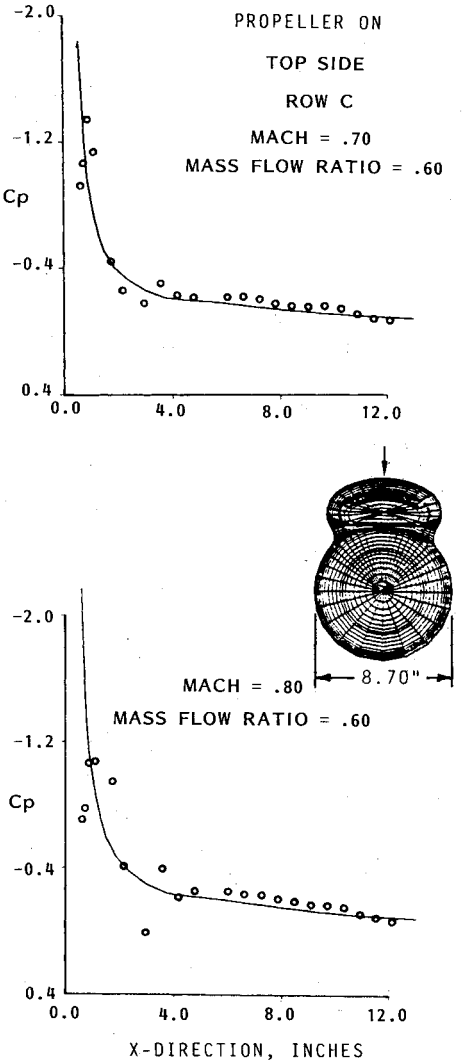

Fig. 8 Pressure distributions for single-scoop inlet with boundary-layer diverter, effect of Mach number.

higher (more negative) pressure coefficient levels on the leeward side of the scoop, due to the propeller-induced swirl, are predicted very well by the theory.

The best correlation with experiment was obtained for the single-scoop inlet with boundary-layer diverter because the effects of the propeller-hub boundary layer were minimized by raising the scoop off the nacelle body. The effect of the propeller is presented in Fig. 6. In comparison to the propeller-off case, the inlet has higher negative pressure peaks on the leeward side of the scoop (row E pressure taps) with the propeller on because of the propeller-induced swirl angle. This effectively places the leeward side of the scoop at a higher angle of attack, while the windward side of the scoop is effectively at a lower angle of attack. On the top of the scoop, the effect of the propeller is minimal. The inclusion of pressure rise across the propeller disk clearly improves correlation with experiment, as is illustrated in Fig. 6 by comparison of the dashed and solid lines. The latter results include this effect. All of these effects are remarkably well predicted by the theory, considering that the method is completely inviscid. Only on the windward side forward on the scoop is there any disagreement, much as with the disagreement noted for the flush inlet.

The correlation presented in Fig. 7 shows the effect of increasing mass flow ratio. The lower pressure peaks shown on the top of the scoop indicate that spillage and velocities over the inlet are reduced, as would be expected.

The effect of Mach number is presented in Fig. 8, with a comparison of data for Mach numbers of 0.70 and 0.80. The data for a Mach number of 0.70 are similar to that shown for a Mach number of 0.60 in Fig. 6. The QUADPAN calculation for linearized compressible flow typically predicts higher negative pressure peaks with increasing Mach number. However, at a Mach number of 0.80, shocks occur, and they drop the measured pressure peaks and alter the pressure distribution on the front of the inlet. QUADPAN cannot predict this nonlinear Mach effect.

Table 1 Percentage reduction of propeller vibratory stresses for aft-mounted single-scoop inlet

Mach	Mass flow ratio	rpm	Total stress, %	1P stress, %	2P stress, %
0.8	0.81	8204	38	29	36

The agreement in the preceding correlations validates the panel method/propeller theory and indicates its capability for inlet design. Based on the predictions, the inlet lip and cowl may be contoured to minimize high negative pressure peaks and reduce the possibility of shocks. This theory was applied to a complete propfan nacelle aircraft installation and was further validated with test data from that configuration.[7]

Mutual Nacelle-Inlet/Propeller Interactions

In considering interactions between the inlet and propeller, the first step is to assess the effect of the inlet on the pro-

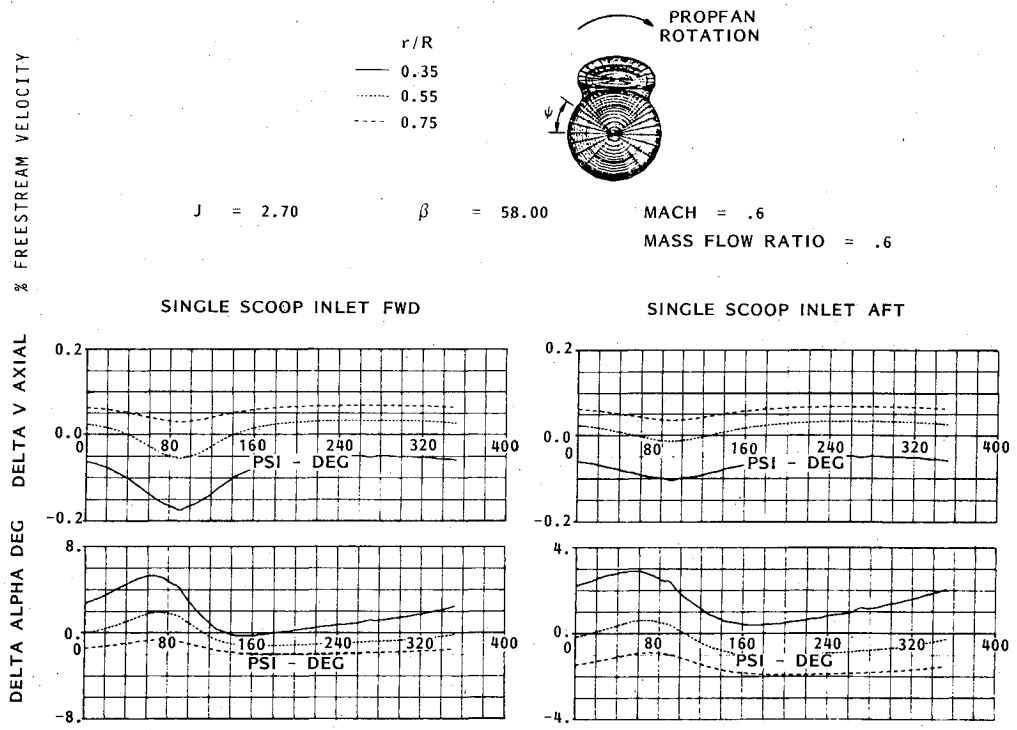

Fig. 9 Effect of inlet on propeller plane axial velocities and blade angle of attack.

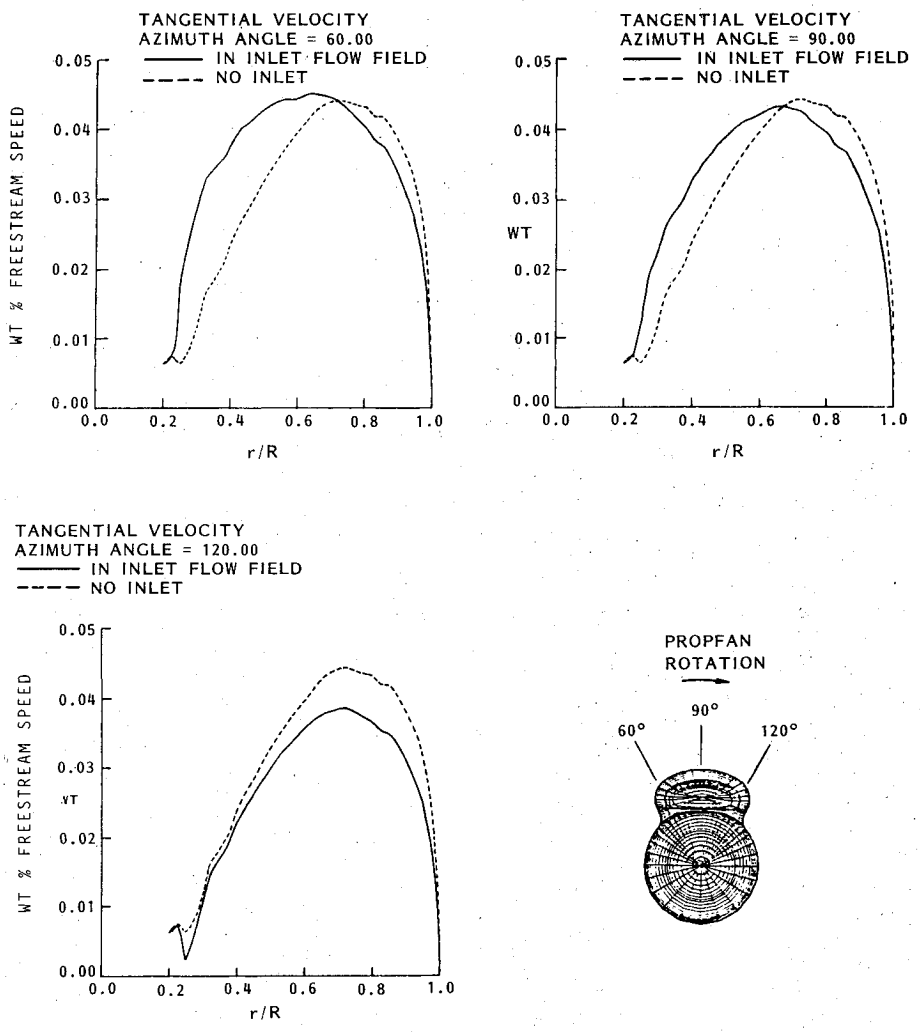

Fig. 10 Propeller-induced tangential velocity with and without single-scoop inlet.

peller. Next, one can consider the effect of the propeller, with its performance modified by the presence of the inlet, on nacelle surface pressures. The effect of the nacelle interference flowfield on the propeller is demonstrated by calculating the change of axial velocity and local propeller angle of attack in the propeller plane for different fore and aft locations of the inlet. Lockheed's PROPVRTX program,[5] described previously, was used for this and also for calculating the change in propeller-induced axial and tangential velocities due to the presence of the inlet scoop. As mentioned previously, two inlet positions were tested for the single-scoop inlet with boundary-layer diverter. The calculated change in the flowfield at the propeller plane is presented in Fig. 9 for the forward position of the inlet (11% in terms of propeller diameters behind the propeller axis). The change in axial velocity, as a percentage of freestream velocity, and local propeller blade angle of attack is shown for three propeller radii around the azimuth swept by the propeller. As would be expected, the presence of the inlet causes a reduction in axial velocity in front of it. The propeller blade angle of attack effectively increases as the propeller rotates toward the inlet, because the tangential component of the flow spilling out of the inlet is coming at the propeller blade. After the propeller passes the inlet, the flow spilling out of the inlet goes in the direction of propeller blade rotation, and the angle of attack is correspondingly reduced.

Figure 9 also presents a similar analysis for the aft-mounted inlet, which is located 20% behind the propeller in terms of propeller diameters. Once again, the axial velocity is reduced and the propeller angle of attack increased in front of the inlet, but the change in the flowfield is considerably less than that for the forward-mounted inlet. This effect is confirmed by examining SR-3 blade root bending vibratory stress measurements, as reported by Hamilton Standard.[8] The stresses were determined by a strain gage located at the propeller root. The results show that the total vibratory stress was reduced by 38% for the aft-mounted inlet, and similar reductions were noted for the 1P and 2P components of vibratory stress, as shown in Table 1.

These results serve to highlight a very important design consideration in terms of inlet placement. From the standpoint of pressure recovery, it is advantageous to place the inlet as close as possible to the propeller,[1] but the stresses imposed on the propeller may be unacceptable in that position. Therefore, the inlet must be moved aft until the cyclic stresses on the propeller are acceptable. The preceding analysis assisted in locating the inlet for a propfan nacelle aircraft installation.[7]

Calculation of nacelle interference flowfields provided the required data to use with the PROPVRTX program to obtain azimuthal variations in propeller slipstream properties at the propeller plane. A variation of tangential velocity, as a percentage of freestream velocity, induced over the length of a propeller blade, with and without the three-dimensional inlet interference flowfield, is shown in Fig. 10. This is for propeller blade positions approaching the inlet, directly in front of the inlet, and after passing the inlet. A significant

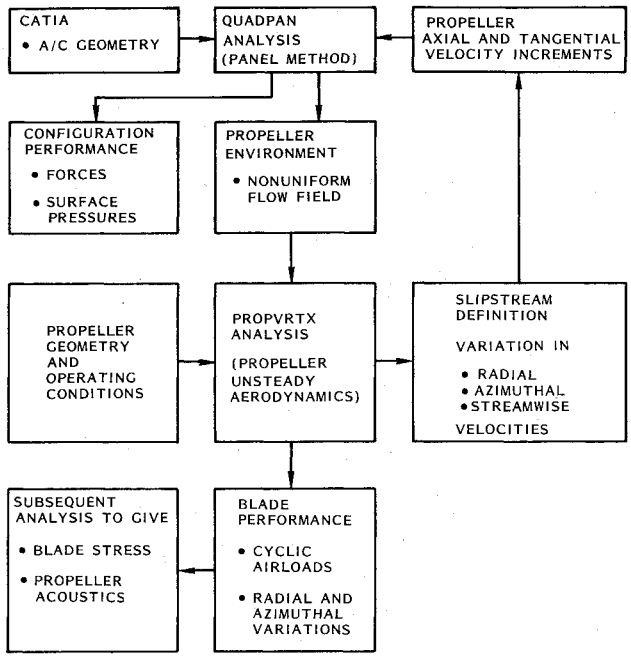

Fig. 11 Propeller/nacelle mutual interactions.

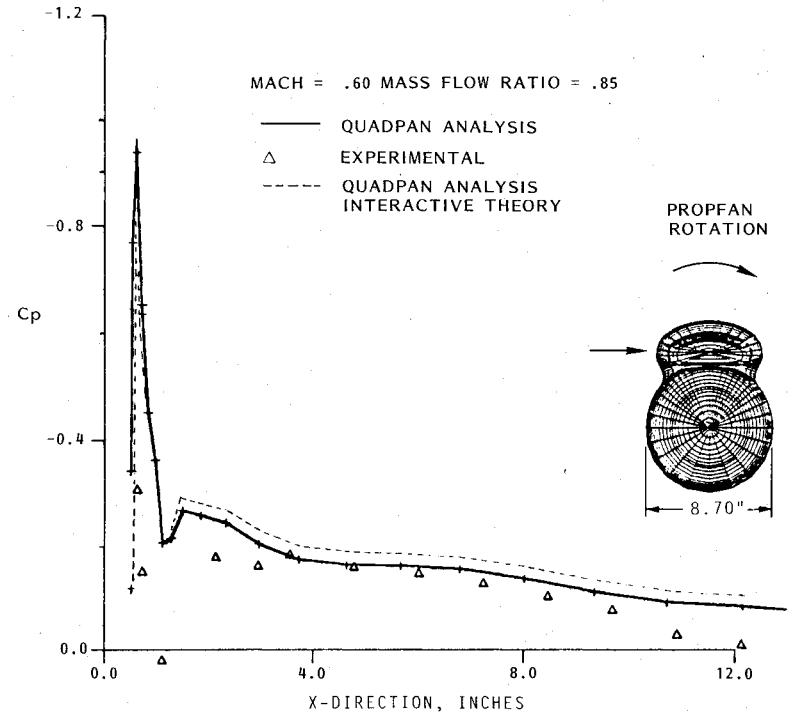

Fig. 12 Pressure distribution for single-scoop inlet, windward side of scoop, with propeller/nacelle mutual interactions included.

increase in induced tangential velocity is evident for the inboard sections of the propeller blade as it approaches and passes the inlet. Induced axial velocity along the propeller blade also varies in this same manner. The increment in axial and tangential velocities induced by the propeller with and without the inlet is then included in the propeller slipstream model along with the isolated propeller-induced velocities, but the downstream development of the slipstream is still based on the "rigid" model presently incorporated in the code. As shown in a flowchart of the interactive propeller nacelle calculation (Fig. 11), these combined velocities are reapplied as a boundary condition on the nacelle surface.

Although the nacelle presence alters the propeller flowfield and performance, the calculated effect of this on nacelle surface pressures is negligible, as the axial and tangential velocities change in roughly the same proportion and thereby maintain flow angularity. Also, as this is a quasi-steady theory, the effects of certain propeller/nacelle interactions at high propeller rotational speeds are not considered. Figure 12 presents this calculation for the single-scoop inlet with boundary-layer diverter and shows the slight change in nacelle surface pressures from those calculated with the isolated propeller slipstream. The negative pressure peak on the front of the inlet is somewhat reduced but not enough to account for the discrepancy, possibly due to a localized unsteady propeller/inlet interaction noted previously on the windward side of the cowl. Farther back on the cowl, the pressures are slightly more negative than for the isolated propeller calculation. This is because of an additional axial velocity increment induced by the propeller on the windward side of the cowl that increases in the downstream direction because of slipstream contraction. Although this procedure could be carried through several iterations by successively recalculating the nacelle flowfield and propeller performance, the results of Fig. 12 indicate that no more than one iteration is necessary.

Conclusions

Correlations of theory and experiment have been presented for a number of different propfan-nacelle configurations. The experimental data are unique for inlet testing in that the large number of pressure taps installed on the nacelle surface permit detailed correlation over a range of Mach numbers and mass flow ratios. Interactions between the propeller and nacelle have also been considered. The following conclusions are drawn.

1) The present theoretical methods will provide good predictions of nacelle surface pressures with proper geometrical representation of the nacelle and proper definition of the propeller slipstream.

2) The effect of the inlet flowfield on the propeller is significant in terms of propeller stresses for an inlet close to the propeller.

3) The effect on nacelle surface pressures of the change in propeller performance, due to the inlet interference flowfield, is not significant, at least as shown by a quasi-steady analysis.

4) The importance of computational methods is demonstrated for optimizing the location of the inlet behind the propeller and for contouring the inlet lip and cowl to minimize high negative pressure peaks there.

5) Good predictions can be obtained up to subsonic Mach numbers of 0.70, but nonlinear compressibility effects, including shocks, appear at higher Mach numbers. Transonic computer codes should be used for such cases, but the required computational grids are difficult to establish for configurations such as inlets with boundary-layer diverters.

References

[1]Hancock, J. P., Lyman, V., and Pennock, A. P., "Analysis of Results from Wind Tunnel Tests of Inlets for an Advanced Turboprop Nacelle Installation," NASA CR 174937, June 1986.

[2]Little, B. H. Jr. and Hinson, B. L., "Inlet Design for High-Speed Propfans," SAE Technical Paper 821359, 1982.

[3]Hinson, B. L., "Design and Experimental Evaluation of Propfan Inlets," SAE Technical Paper 841477, Oct. 1984.

[4]Coopersmith, R. M., Youngren, H. H., and Bouchard, E. E., "Quadrilateral Element Panel Method (QUADPAN)," User's Manual Version 3.2, Lockheed-California Co., Burbank, LR 30563, 1984.

[5]Aljabri, A. S., "Prediction of Propeller Performance and Loading in Uniform and Non-uniform Flowfields," M.S. Thesis, The Pennsylvania State University, University Park, Nov. 1978.

[6]Rohrbach, C., Metzger, F., Black, D., and Ladden, R., "Evaluation of Wind Tunnel Performance Testings of an Advanced 45 Degree Swept Eight Bladed Propeller at Mach Numbers From 0.45 to 0.85," NASA CR 3505, March 1982.

[7]Aljabri, A. S., Lyman, V., and Parker, R. J., "Evaluation of Propeller/Nacelle Interactions in the PTA Program," AIAA Paper 86-1552, June 1986.

[8]Bansal, P. N., "Experimental and Analytical Evaluation of the Effects of Simulated Engine Inlets on the Blade Vibratory Stresses of the SR-3 Model Propfan," NASA CR 174959, Sept. 1985.